Neoplasia • Vol. 9, No. 5, May 2007, pp. 358–369 359

www.neoplasia.com

4-IBP, a σ_1 Receptor Agonist, Decreases the Migration of Human Cancer Cells, Including Glioblastoma Cells, *In Vitro* and Sensitizes Them *In Vitro* and *In Vivo* to Cytotoxic Insults of Proapoptotic and Proautophagic Drugs[1]

Véronique Mégalizzi, Véronique Mathieu*,[2], Tatjana Mijatovic[‡], Philippe Gailly[§], Olivier Debeir[¶], Nancy De Neve[‡], Marc Van Damme*, Gianluca Bontempi[#], Benjamin Haibe-Kains[#,**], Christine Decaestecker*,[2], Yasuko Kondo[†], Robert Kiss*,[2] and Florence Lefranc*,[††,2]*

*Laboratoire de Toxicologie, Institut de Pharmacie, Université Libre de Bruxelles, Brussels, Belgium; [†]Department of Neurosurgery, University of Texas M. D. Anderson Cancer Center, Houston, TX, USA; [‡]Unibioscreen SA, Brussels, Belgium; [§]Département de Physiologie et de Pharmacologie, Université catholique de Louvain, Brussels, Belgium; [¶]Service des Systèmes Logiques et Numériques, Faculté des Sciences Appliquées, Université Libre de Bruxelles, Brussels, Belgium; [#]Machine Learning Group, Department of Computer Science, Université Libre de Bruxelles, Brussels, Belgium; **MicroArray Unit, Jules Bordet Institute, Brussels, Belgium; [††]Département de Neurochirurgie, Cliniques Universitaires de Bruxelles, Hôpital Erasme, Université Libre de Bruxelles, Brussels, Belgium

Abstract

Although the molecular function of σ receptors has not been fully defined and the natural ligand(s) is still not known, there is increasing evidence that these receptors and their ligands might play a significant role in cancer biology. 4-(*N*-benzylpiperidin-4-yl)-4-iodobenzamide (4-IBP), a selective σ_1 agonist, has been used to investigate whether this compound is able to modify: 1) *in vitro* the migration and proliferation of human cancer cells; 2) *in vitro* the sensitivity of human glioblastoma cells to cytotoxic drugs; and 3) *in vivo* in orthotopic glioblastoma and non–small cell lung carcinoma (NSCLC) models the survival of mice co-administered cytotoxic agents. 4-IBP has revealed weak antiproliferative effects on human U373-MG glioblastoma and C32 melanoma cells but induced marked concentration-dependent decreases in the growth of human A549 NSCLC and PC3 prostate cancer cells. The compound was also significantly antimigratory in all four cancer cell lines. This may result, at least in U373-MG cells, from modifications to the actin cytoskeleton. 4-IBP modified the sensitivity of U373-MG cells *in vitro* to proapoptotic lomustin and proautophagic temozolomide, and markedly decreased the expression of two proteins involved in drug resistance: glucosylceramide synthase and Rho guanine nucleotide dissociation inhibitor. *In vivo*, 4-IBP increased the antitumor effects of temozolomide and irinotecan in immunodeficient mice that were orthotopically grafted with invasive cancer cells.

Neoplasia (2007) **9,** 358–369

Keywords: Cancer cell migration, σ receptor, Rho GDI, glucosylceramide synthase, orthotopic xenografts.

Introduction

σ Receptors have been studied mostly with respect to their functions within the central nervous system [1–4]. Additional functions of σ receptors in connection with the motor, endocrine, and immune systems have also been suggested [5,6]. These σ receptors, however, have also been found to be overabundant in many tumors of neural and non-neural origin [7] and might, therefore, play a significant role in cancer biology [4]. They were first described as a subtype of opiate receptors [8], but they were later distinguished from them by the development of selective σ ligands [9]. Indeed, radioligand-binding studies subsequently indicated that there are at least three, and possibly more, subtypes of σ receptors, designated as σ_1, σ_2, and σ_3 [3]. Radioligand-binding data have also demonstrated that the σ_1 receptor is related both to a sterol isomerase, which is involved in the cholesterol biosynthesis pathway [3,6,10], and to SR31747-binding protein-2, with which it shares a high level of homology but which is of unknown function [11]. The σ_1 receptor has been cloned [12,13], and five transcription variants are known (Gene

Address all correspondence to: Robert Kiss, Laboratory of Toxicology, Institute of Pharmacy, Free University of Brussels, Campus de la Plaine CP205/1, Boulevard du Triomphe, 1050 Brussels, Belgium. E-mail: rkiss@ulb.ac.be

[1]The present work has been carried out based on grants awarded by the *Fonds Yvonne Boël* (Brussels, Belgium) and the *Fonds National de la Recherche Scientifique* (FNRS; Brussels, Belgium).

[2]Véronique Mathieu is the holder of a *Grant Télévie* from the Belgian National Funds for Fundamental Research (FNRS, Belgium), F.L. is a Clinical Research Fellow with the FNRS, and C.D. and R.K. are Senior Research Associate and Director of Research, respectively, with the FNRS.

Received 16 January 2007; Revised 3 April 2007; Accepted 4 April 2007.

DOI 10.1593/neo.07130

Bank Data Base: NM_005866, NM_147157, NM_147158, NM_147159, and NM_147160).

Both σ_1 and σ_2 receptor subtypes are highly expressed in tumor cell lines from various human cancers, including small cell lung carcinoma and non–small cell lung carcinoma (NSCLC), renal carcinomas, colon carcinomas, sarcomas, brain tumors, breast cancers, melanomas, and prostate cancers [4]. Small molecules that bind to the σ receptor (σ ligands or σ-modulating drugs) have many potential functions [10] and are used in diagnostic tumor imaging [14]. Such compounds are also able to modify the growth rates of human cancer cell lines both *in vitro* [6,15–17] and *in vivo* [18,19]. These drug-induced decreases in cell growth rate seem to occur through rises in intracellular calcium ($[Ca^{2+}]_i$) and through apoptosis [17]. It has also been suggested that these effects on cell growth and apoptosis occur by the sphingolipid pathway [20].

Migratory (and metastatic) cancer cells are resistant to apoptosis, as revealed in ever more publications [21]. However, decreasing the levels of migration of tumor cells can restore a certain level of sensitivity to cytotoxic insult [22]. Although several reports have emphasized a potential role for the σ receptor and/or σ-modulating drugs in reducing cancer cell proliferation and/or increasing cancer cell death, no study has been published to date, at least to the best of our knowledge, concerning their potential role either in cancer cell migration or in the modulation of the effects of proapoptotic and proautophagic drugs. In this context, 4-(*N*-benzylpiperidin-4-yl)-4-iodobenzamide (4-IBP), a selective σ_1 agonist [23,24] with a high level of affinity for the σ_1 receptor (K_i = 1.7 nM) and a moderate affinity for the σ_2 receptor (K_i = 25.2 nM) [10,25], was used to investigate whether targeting the σ_1 receptor could modify *in vitro* the migration rates of human cancer cells and increase *in vitro* and *in vivo* the sensitivity of metastasizing human A549 NSCLC cells and infiltrating human glioblastoma cells to cytotoxic insults of either proapoptotic or proautophagic drugs. A σ_1 receptor agonist, rather than an antagonist, was used because we wanted to mimic a biologic situation in which the σ_1 receptor is activated, as it might be, by yet to be identified endogenous ligands.

Materials and Methods

Cell Lines

Four human cancer cell lines—PC3 prostate (ATCC code CRL-1435), A549 NSCLC (CLL-185), C32 melanoma (CRL-1585), and U373-MG glioblastoma (HTB-17)—were obtained from the American Type Culture Collection (Manassas, VA) and thereafter maintained *in vitro* in accordance with their recommendations.

Compounds

4-IBP was obtained from Tocris Bioscience (Bristol, UK). Temozolomide was obtained from Schering Plough (Brussels, Belgium), lomustin was from Medac (Hamburg, Germany), and irinotecan (IRI) was from Sanofi-Aventis (Paris, France).

Standard Reverse Transcription–Polymerase Chain Reaction (RT-PCR) for the Determination of σ_1 Receptor Variants in Human Cancer Cells

The procedure used was identical to that described previously [26]. As detailed in Figure 1*A* and its legend, two pairs of primers were used to evidence the presence or the absence of five σ_1 receptor variants in human C32 melanoma, U373-MG glioblastoma multiforme (GBM), A549 NSCLC, and PC3 prostate cancer cell lines:

- Primer P1: 5′-gccttctctcgtctgatc-3′ (forward) and 5′-cgtgtactaccgtctcc-3′ (reverse)
- Primer P2: 5′-ggagacggtagtacacg-3′ (forward) and 5′-agcataggagcgaagagt-3′ (reverse).

Kekuda et al. [13] originally cloned functional σ_1 receptor cDNA from a human placental choriocarcinoma cell (JAR) library using a guinea pig–specific mRNA RT-PCR product [12]. Prasad et al. [27] then detailed the structure and organization of the human gene coding for this σ_1 receptor. The gene contains four exons interrupted by three introns. A number of researchers then submitted various transcription variants of this mRNA directly to the Gene Bank Data Base (without further scientific publication). These variants are numbered from 1 to 5 and referenced as NM_005866, NM_147157, NM_147158, NM_147159, and NM_147160, respectively. As 4-IBP may bind differentially to these five σ_1 receptor variants [10], an RT-PCR approach was used to first investigate their expression pattern in the four designated cancer cell lines. Based on published sequences for the above splice variants, primer set P2 was chosen as it recognizes all five of the described splice variants in the common region (*exon 4*; Figure 1*A*) and so yields one single amplification fragment (Figure 1, *C* and *D*). Conversely, the use of primer set P1 allowed distinction to be made between V1, V3 + V4, and V2 + V5 (Figure 1, *B* and *D*). Any further distinction between the different variants was technically impossible because sequence differences were too small to enable correct primer design and visible differences in the size of the amplified fragment to be ascertained.

Protein Expression and Activity Measurements

Western blot analysis and immunofluorescence analyses were performed as detailed previously [26,28]. The proteins were detected by the following primary antibodies: anti-ORP150 (dilution 1/100; IBL, Minneapolis, MN), anti-GRP78 (dilution 1/250; Sigma-Aldrich, Bornem, Belgium), anti-p53 (dilution 1/1000; Calbiochem VWR International, Leuven, Belgium), anti–Beclin-1 (dilution 1/250; BD Transduction Laboratories, Erembodegem, Belgium), anti-Hsp70 (dilution 1/500; Cell Signaling, Bioké, Leiden, The Netherlands), anti–Rho guanine nucleotide dissociation inhibitor (Rho GDI; dilution 1/500; Cell Signaling), and anti–glucosylceramide synthase (GCS; dilution, 5 μg/ml; Exalpha Biologicals, Inc., Mahnard, MA). The levels of both total and phospho p85-PI3K and Akt expressions were determined using the Fast Activated Cell–Based ELISA Kit (Active Motif, Rixensart, Belgium).

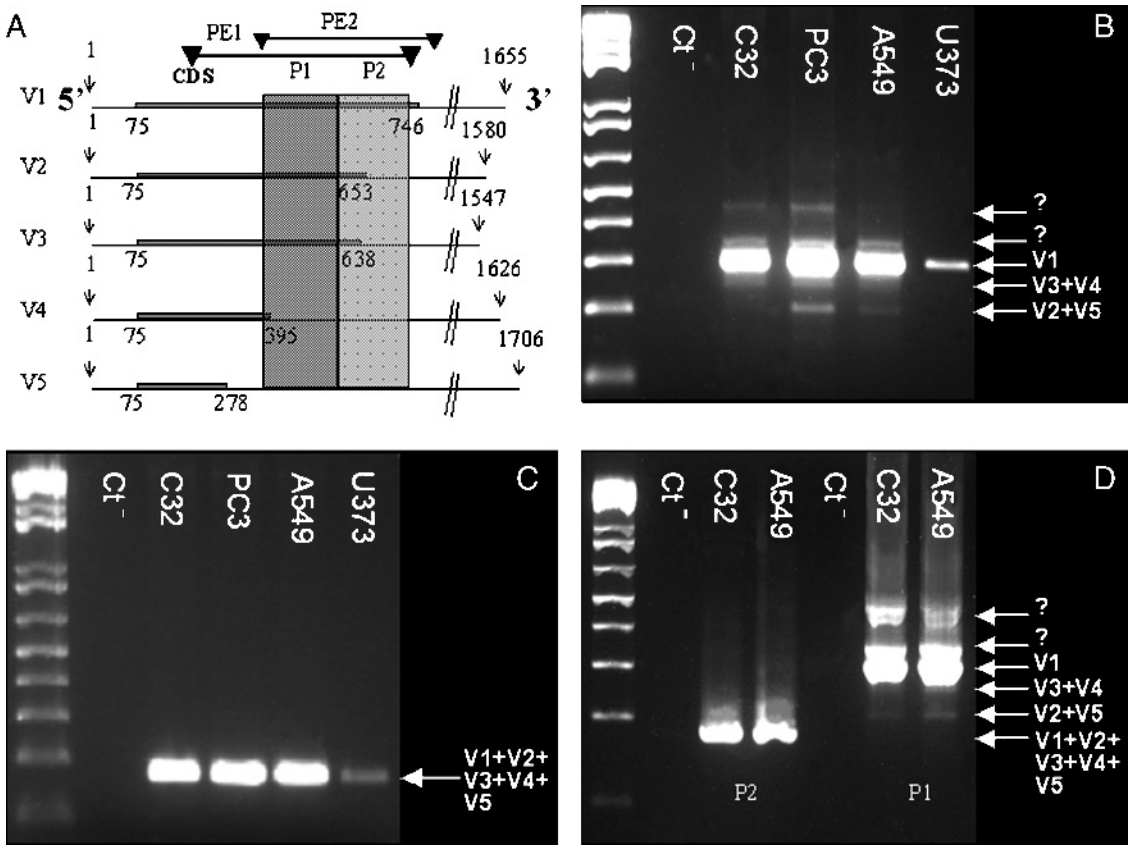

Figure 1. *Expression of the splice variants of σ_1 receptor mRNA (V1–V5) in four different human cancer cell lines, namely, melanoma (C32), refractory prostate (PC3), NSCLC (A549), and glioma (U373-MG) cells, as assessed by RT-PCR analyses. (A) Schematic representation of the five different splice variants of σ_1 receptor mRNA, with the exact sites targeted by two different pairs of primers (P1 and P2) used to investigate the expression patterns of the splice variants. CDS = mRNA-coding region. Primer positions are outlined by black (P1) and gray (P2) hatched boxes, respectively. (B and C) The detection of splice variants of σ_1 receptor mRNA by RT-PCR using primer pairs P1 and P2, respectively. (D) The detection of splice variants of σ_1 receptor mRNA by RT-PCR using primer pairs P2 and P1, respectively, and carried out on purified fragments isolated after PCR performed with "external primers" (PE1 and PE2). (B–D) First lane: 1-kb plus DNA size ladder; Ct⁻: nontemplate control (H_2O). White arrows indicate the positions of different amplified splice variants. (?) Nonspecified amplification fragments (for RT-PCR experimental details, see Materials and Methods section).*

Determination of Apoptosis and Autophagy

Apoptosis was analyzed by flow cytometry using the terminal deoxynucleotidyl transferase deoxyuridine triphosphate nick-end labeline (TUNEL) technique, as well as by the analysis of the cleavage pattern of poly(ADP-ribose) polymerase (PARP), which was assessed by Western blot analysis using anti-PARP antibody (1/250; BD PharMingen, Erembodegem, Belgium), as detailed previously [26]. Autophagy was analyzed by the staining of acidic vesicular organelles with acridine orange (purchased from Polysciences, Warrington, PA), as detailed elsewhere [29]. Western blot analyses of light chain 3 (LC3), a specific marker of autophagy, were also performed with a rabbit–anti-LC3 antibody raised in our laboratory [29]. Flow cytometry analyses were performed immediately after a staining reaction on an Epics XL.MCL flow cytometer (Beckman Coulter, Miami, FL) equipped with a 488-nm argon laser.

In Vitro *Characterization of 4-IBP–Induced Effects on the Growth Rates of Human Cancer Cell Populations*

The influence of 4-IBP on the overall growth rates of the four human cancer cell lines under study was determined by colorimetric MTT assay, as previously described [28]. Each experiment was conducted in sextuplicate. Nine 4-IBP concentrations ranging from 10^{-9} to 10^{-5} M (with semilog increases in concentration) were evaluated. Cancer cells had been incubated with 4-IBP for 3 days before overall growth rates were determined.

In Vitro *Characterization of 4-IBP Antimigratory Activity in Human Cancer Cells*

Human cell motility was characterized using computer-assisted phase-contrast microscopy to quantitatively determine the levels of migration of individual human cancer cells *in vitro*, as described previously [30]. The effect of 4-IBP on cell motility levels in C32, PC3, A549, and U373-MG human cancer cell lines was investigated at 1, 10, and 100 nM. Figure 2*C* shows a typical analysis based on individual cell trajectories, established by a cell-tracking algorithm based on an image series acquired during a cell migration experiment. The greatest linear distance between a cell's starting point and the farthest point reached in its trajectory, the maximum relative distance from the point of origin (MRDO), was the quantitative variable [30] used

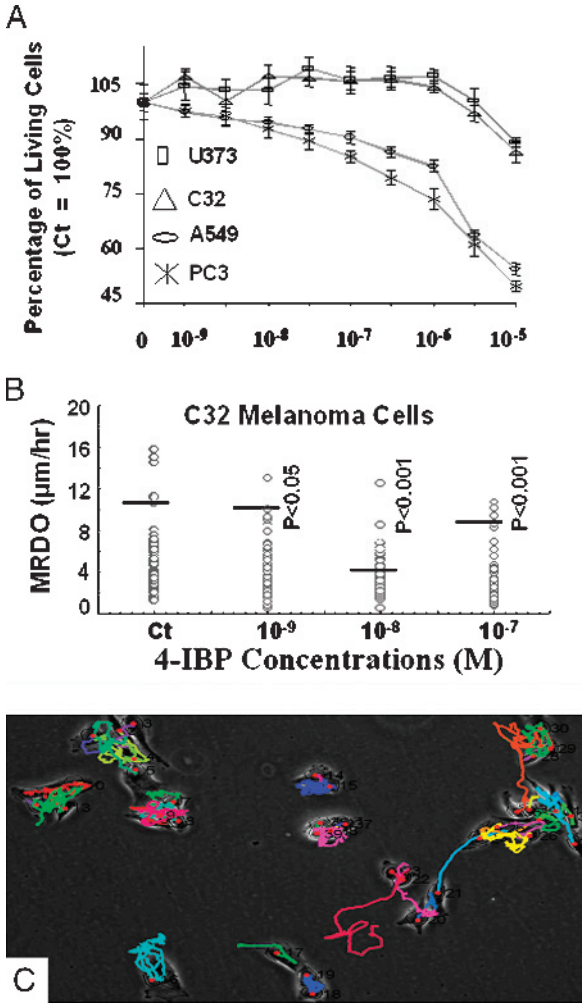

Figure 2. *Evaluation of the antiproliferative and antimotility activities of 4-IBP in cancer cells. (A) Percentages of living cells assessed by the colorimetric MTT assay in four human cancer cell lines (U373-MG, C32, A549, and PC3). The data are shown as mean ± standard error with respect to the 4-IBP concentrations used (see x-axis). (B) Distribution of MRDO values obtained for C32 cells treated with increasing 4-IBP concentrations (see x-axis) and those left untreated (Ct). The data show individual values (dotted) and corresponding medians (horizontal bars). (C) Typical quantification experiment of the motility levels of individual cells by establishing the trajectory of each cell centroid and by quantifying the MRDO variable (i.e., maximum distance covered by a cell normalized by its observation time, expressed in µm/hr).*

to characterize compound-mediated effects on cancer cell migration.

Characterization of the Organization of Actin Cytoskeleton in Human U373-MG Glioblastoma Cells

Fluorescent phallacidin conjugated with Alexa Fluor 488 fluorochrome (Molecular Probes, Inc., Eugene, OR) was selected to label fibrillar actin, whereas Alexa Fluor 594–conjugated DNAseI (Molecular Probes, Inc.) was used to stain globular actin. As described previously [31], U373-MG GBM cells were cultured for various periods in the absence (controls) or in the presence of 1 and 10 nM 4-IBP on glass coverslips before fluorescence staining. The fluorescence intensity of fluorochromes was quantified by a computer-assisted fluorescent Olympus AX70 microscope (Omnilabo, Antwerp, Belgium) equipped with a Megaview2 digital camera and analySIS software (Soft Imaging System, Munster, Germany). One hundred cells were quantified under each experimental condition. Cell morphology was also characterized with respect to four quantitative features provided by the analySIS software and comprised cell area, sphericity, elongation, and morphologic pattern.

Intracellular Calcium Measurements in Human U373-MG Glioblastoma Cells

The procedure used here was identical to that described previously [32]. The intensity of fluorescence was recorded over the entire surface of single cells, and $[Ca^{2+}]_i$ was then calculated from the ratio of the intensities of fluorescence excited at two defined wavelengths. For this purpose, a standard intracellular calibration procedure was performed after cell permeabilization with 5 µM ionomycin.

In Vitro *Scratch Wound Assay*

U373-MG glioblastoma cells were grown to confluence in six-well dishes [21,26] before being pretreated with 10 nM 4-IBP for 1, 3, 7, or 24 hours in a serum-restricted medium (5%). Scratch wounds were made by creating a denuded linear area with a pipette tip [26]. The cells were washed twice with phosphate-buffered saline before their incubation with a cytotoxic agent (lomustin or temozolomide) at 1 and 10 µM in a serum-restricted medium for 16 additional hours of post–4-IBP treatment. Four fields per well were photographed twice daily until wound healing was observed in appropriate controls. A software developed in our laboratory was used to quantify the percentage of the scratch wound area filled by cells [21,26] over the period of the experiment.

Genomic Analyses

U373-MG GBM cells were either left untreated or treated with 10 nM 4-IBP for 12 hours. RNA extraction and determination of the quality and integrity of extracted RNA were assessed as detailed previously [26]. Full genome analyses were performed at the VIB MicroArray Facility (UZ Gasthuisberg, Catholic University of Leuven, Leuven, Belgium) for which purpose Affymetrix Human Genome U133 set Plus 2.0 (High Wycome, Buckinghamshire, UK) was used.

4-IBP Treatment of Orthotopic Xenografts of Human U373-MG Glioblastoma in the Brains of Immunodeficient Mice

The U373-MG GBM model was used to characterize the *in vivo* antitumor effects of 4-IBP because: 1) these cells were found to have only one σ_1 receptor variant (Figure 1); 2) they are resistant to proapoptotic cytotoxic drugs [33], as are GBM patients [22]; 3) they are sensitive to proautophagic effects of temozolomide [29,33], as are GBM patients [34]; and 4) tumor debulking by surgery is of little, if any, therapeutic benefit in the case of immunodeficient mice bearing orthotopic xenografts of the U373-MG GBM model in their brains [35]. Orthotopic xenografts of human U373-MG GBM were obtained by grafting 2 million U373-MG cells into the left

temporal lobes of 8-week-old female nu/nu mice (21–23 g; Iffa Credo, Charles Rivers, Arbresle, France), as detailed previously [31,35]. Forty-four mice grafted with glioblastoma cells in this manner were randomly assigned to four treatment groups of 11 mice on day 10 posttumor graft and then on day 14 were treated as follows: Group 1 mice (the control) were grafted subcutaneously with an osmotic minipump (Alzet; Charles River Laboratories, L'Arbresle, France) that delivered the vehicle 4-IBP [saline with 1% dimethyl sulfoxide (DMSO)] continuously through a catheter into the third ventricle over a period of 28 days [35]. Group 2 mice received treatment identical to that in Group 1, except that the minipumps delivered a 4-IBP solution (in saline containing 1% DMSO) at a dose of 2 mg/kg. This dose had been chosen based on the *in vivo* study published by Bermack and Debonnel [10]. Group 3 mice received 12 intravenous injections of temozolomide at a dose of 40 mg/kg. The 12 injections were performed thrice a week (on Mondays, Wednesdays, and Fridays) over four consecutive weeks, with the first injection falling on the 21st day post–tumor graft. Group 4 animals received a combination of the treatments described for Groups 2 and 3.

4-IBP Treatment of Orthotopic Xenografts of Human A549 NSCLC in the Lungs of Immunodeficient Mice

The human A549 NSCLC model was investigated because A549 NSCLC cells are chemoresistant and produce brain and liver metastases in nude mice [36]. Orthotopic xenografts of human A549 NSCLC were obtained by grafting 2 million A549 NSCLC cells into the right lung of 8-week-old female nu/nu mice (21–23 g; Iffa Credo, Charles Rivers), as detailed previously [36]. Grafted mice were randomly allocated to treatment groups, as detailed above. Group 1 received 12 intravenous injections of 50 μl of saline and acted as the control group, with the first injection starting on the seventh day posttumor graft. The injections were performed thrice a week over four consecutive weeks. Under an identical regimen, Group 2 received 12 intravenous injections of a 4-IBP solution at a dose of 2 mg/kg. Group 3 received 12 intravenous injections of an IRI solution at a dose of 10 mg/kg. IRI was chosen given its proapoptotic effects. 4-IBP treatment started on day 7 posttumor graft, whereas IRI treatment started on day 14 postgraft. The IRI treatment was chosen based on data previously obtained [36]. Group 4 received the combined treatment described for mice in Groups 2 and 3.

All *in vivo* experiments described in the current study were performed based on authorization no. LA1230509 of the Animal Ethics Committee of the Federal Department of Health, Nutritional Safety, and the Environment (Belgium).

Data Analyses

Statistical comparisons were made by the Kruskal-Wallis test (a nonparametric one-way analysis of variance). Where this test revealed some significant differences, treatment groups were then compared by applying the Mann-Whitney test. Survival analyses were carried out by Kaplan-Meier analyses. All statistical analyses were performed using Statistica (Statsoft, Tulsa, OK).

Results

Identification of σ_1 Receptors in Human Cancer Cells

As shown in Figure 1, *B–D*, the four cancer cell lines under study displayed different patterns of expression in the σ_1 receptor splice variants: U373-MG GBM cells did not express any variant other than V1; C32 melanoma cells expressed V1, V3 + V4, and, to a lesser extent, V2 + V5; and A549 NSCLC and PC3 prostate cancer cells expressed all five variants.

In Vitro *Characterization of 4-IBP–Mediated Effects on the Overall Growth of Human Cancer Cell Lines*

4-IBP was found to have weak antiproliferative effects on human U373-MG GBM and C32 melanoma cells (Figure 2*A*). Indeed, even at 10 μM for 3 days, the highest 4-IBP concentration tested, a maximum of only 10% growth inhibition was observed in these two cell lines. In contrast, 4-IBP induced a concentration-dependent decrease in the growth of human A549 NSCLC and PC3 prostate cancer cells (Figure 2*A*). Thus, A549 and PC3 cells, unlike C32 and U373-MG cells, appear to be susceptible to 4-IBP–provoked cell death, notably at concentrations of $\geq$ 1 μM.

In Vitro *Characterization of 4-IBP–Mediated Effects on Cancer Cell Migration*

Although 4-IBP was found not be antiproliferative at concentrations of up to 10 μM against C32 melanoma cells, the compound was found to have significant antimigratory effects at concentrations between 1 and 100 nM in this cell line, as evidenced by a significant decline in MRDO (Figure 2*B*). Similar antimigratory features were observed with the three other human cancer cell lines investigated: U373-MG GBM (Figure 3*E*), A549 NSCLC (data not shown), and PC3 (data not shown).

Characterization of 4-IBP–Mediated Effects on Cell Morphology and Actin Cytoskeleton Organization

Several steps in the cell migration process in extracellular matrix environments are usually paralleled by marked modifications in cell shape [21,22,37]. Figure 3*A* shows the four quantitative features used to characterize cell morphology. Degree of sphericity, elongation, and morphologic pattern are three complementary variables that permit the evaluation of the roundness of a cell (i.e., the farther is the value from 1, the greater is the likelihood that a cell presents an elongated morphology). In addition, a cell's spread is evaluated by the determination of its area. Although 4-IBP (1–100 nM) significantly modified the migration levels of all four human cancer cell lines investigated, in the present study, over the same concentration range, it left the morphologic patterns of these cells unchanged when compared to controls (data not shown).

Computer-assisted fluorescence microscopy was then used to determine the effects of 1 and 10 nM 4-IBP (concentrations defined as antimigratory but noncytotoxic) on

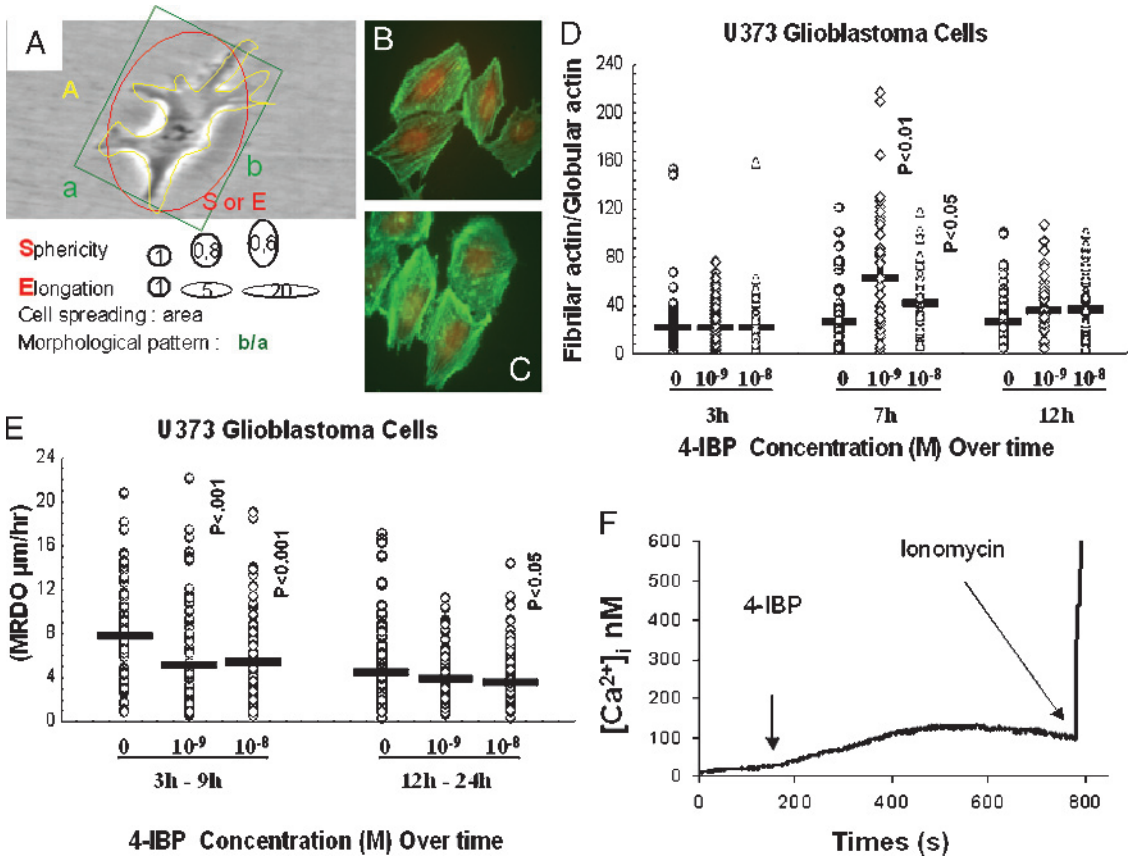

Figure 3. *Evaluation of 4-IBP–induced effects on U373-MG glioblastoma cells. (A) Illustration of the morphologic variables used to evaluate the roundness of a cell (level of sphericity, elongation, and morphologic pattern) and its spread (area). (B and C) Illustration of actin cytoskeleton distribution in control U373-MG cells and in those treated with 1 nM 4-IBP for 7 hours. Fibrillar actin and globular actin appear as green and red fluorescence, respectively. (D and E) Effects of two concentrations of 4-IBP on fibrillar/globular actin ratios and cell motility levels computed over different time periods (as indicated on the x-axis). (F) 4-IBP (10 nM) did not significantly increase $[Ca^{2+}]_i$ in U373-MG GBM cells when compared to ionomycin.*

the organization of the actin cytoskeleton in U373-MG GBM cells. Figure 3*B* illustrates the typical appearance of the actin cytoskeleton in control U373-MG cells in which fibrillar (polymerized) actin appears as green fluorescence and globular (nonpolymerized) actin appears as red fluorescence. Treatment with 1 nM 4-IBP for 7 h increased the level of fibrillar to the detriment of globular actin in human U373-MG cells (Figure 3*C*). Furthermore, quantitative analysis revealed that both 1 and 10 nM 4-IBP induced significant but transient increases in the levels of fibrillar actin in these cells (Figure 3*D*). These effects could lead to a 4-IBP–induced decrease in the levels of migration of these cells (Figure 3*E*). As detailed below, part of 4-IBP–induced modifications to the organization of the actin cytoskeleton occurred through compound-induced reduction in the expression of Rho GDI.

Characterization of 4-IBP–Mediated Effects on Intracellular Calcium Concentration in Human U373-MG Glioblastoma Cells

It appears that 4-IBP may bind to various σ_1 receptor variants [10]. In addition, a structurally diverse range of compounds bind to σ_1 receptors, and a number of these ligands interact with other receptor types [3]. One example of poor specificity is the direct interaction between σ receptor ligands and *N*-methyl-D-aspartate (NMDA) receptors [3,25]. Activation of NMDA receptors is accompanied by a local rise in $[Ca^{2+}]_i$, which is sufficient to trigger a slow and sustained recruitment of actin in dendritic spines during activity-dependent processes underlying neuronal plasticity [38]. Dendritic spines, in fact, contain a specialized cytoskeleton consisting of dynamic actin filaments able to produce rapid changes in their motility and morphology [38]. Modifications to $[Ca^{2+}]_i$ can thus seriously modify the organization of the actin cytoskeleton [39]. Although 4-IBP is a selective σ_1 ligand [25], weak inhibition of cloned NMDA receptor responses in *Xenopus* oocytes has nevertheless been observed with this compound [3]. It was thus considered important to investigate whether the 4-IBP–induced decrease in U373-MG GBM cell migration (Figure 3*E*) and associated changes in actin cytoskeleton organization (Figure 3, *B–D*) resulted from modifications in $[Ca^{2+}]_i$, as encountered in the activation of NMDA receptors [38]. The data obtained at 10 nM strongly suggest that 4-IBP does not modify U373-MG cell migration or the organization of the actin cytoskeleton through modifications in $[Ca^{2+}]_i$ in

this cancer cell line (Figure 3*F*). This, in turn, suggests that 4-IBP–mediated effects on U373-MG cell migration do not occur through the compound's activation of NMDA receptors.

Characterization of the Combined Influences of 4-IBP–Mediated Antimigratory Activity and Cytotoxic Drug–Mediated Effects on the In Vitro *Development of Human U373-MG Glioblastoma Cell Populations*

Migrating human cancer cells, in general [21], and human glioblastoma cells, in particular [22], are protected against apoptosis during migration. Several diverse compounds that are able to decrease the levels of glioblastoma cell migration also restore to these cells a certain level of sensitivity to apoptosis [22,40]. This being the case, the ability of 4-IBP to modify the *in vitro* sensitivity of human U373-MG apoptosis-resistant glioblastoma cells [32] to the cytotoxic effects of either a proapoptotic (lomustin) [41] or a proautophagic (temozolomide) [28] drug was investigated.

Ten nanomolars of 4-IBP, when added to U373-MG cells in the scratch wound assay 1 to 7 hours before the addition of lomustin (1 and 10 μM) or temozolomide (1 and 10 μM), resulted in significant ($P < .01$ to $P < .001$) sensitization of these glioblastoma cells to the proapoptotic effects of 10 μM lomustin (Figure 4*A*) or to the proautophagic effects of 1 and 10 μM temozolomide (Figure 4*B*). This sensitization was essentially lost when 4-IBP was added 24 hours before the addition of either cytotoxic agent.

4-IBP Does Not Induce Apoptosis in Human U373-MG Glioblastoma Cells

The intracellular signaling pathways involved in the acquisition of resistance to apoptosis (type I programmed cell death) by migrating glioma cells concern PI3K, Akt, mTOR, and NF-κB [22]. The PI3K and Akt signaling pathways are interlinked in their regulation of cell survival and cell death in human GBM cells [22]. The data in Figure 4, *C* and *D*,

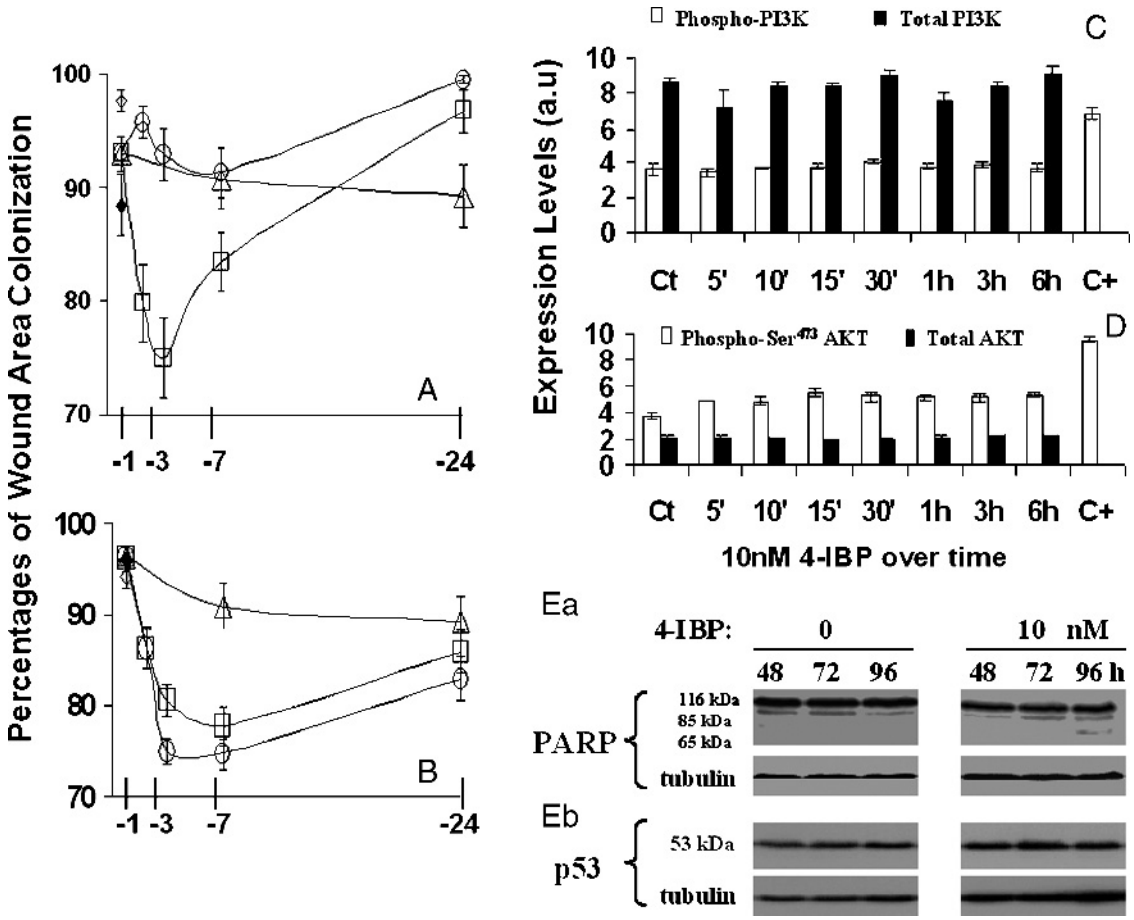

Figure 4. *(A and B) Therapeutic combination of 4-IBP and cytotoxic agents [(A) lomustin and (B) temozolomide] in a scratch wound assay in which colonization by human U373-MG GBM cells of an artificially inflicted wound in a subconfluent cell population was followed over time. (A) and (B) illustrate delay in the wound healing process when U373-MG cells were pretreated with 4-IBP [10 nM; duration exposure varied from 0 (no 4-IBP treatment) to 24 hours on the x-axis] before the cytotoxic insult with lomustin or temozolomide, respectively, used at 1 μM (open dots) or 10 μM (open squares) over 16 hours. Controls were U373-MG cells cultured in the absence of 4-IBP, lomustin, or temozolomide, and were arbitrarily normalized to 100% wound colonization after 24 hours of culture (open triangles in A and B). An additional control was performed for each treatment [i.e., lomustin or temozolomide added alone at 1 μM (black lozenge) or at 10 μM (white lozenge) for 16 hours to the cells, and 4-IBP at 10 nM for 7 and 24 hours of exposure (white triangles)]. (C and D) Evaluation of the levels of expression of total (black bars) and phosphorylated (open bars) p85-PI3K (C) and Akt (D) in U373-MG GBM cells left untreated (Ct) or treated with 10 nM 4-IBP for the periods indicated. The data are expressed as mean ± SEM. Assays were validated using serum-starved U373-MG treated with epidermal growth factor (200 ng/ml) for 10 minutes (C^+). (E) Western blot analyses of PARP cleavage and p53 expression in U373-MG cells left untreated (0) or treated with 10 nM 4-IBP for between 48 and 96 hours.*

indicate that 4-IBP at 10 nM did not modify the pattern of expression of total and phospho p85-PI3K and Akt in U373-MG GMB cells. It is thus unlikely that 4-IBP–mediated sensitization of these cells to the proapoptotic effects of lomustin could relate to compound-mediated modifications to the PI3K/Akt signaling pathway.

The data in Figure 4*Ea* indicate that treatment of U373-MG cells with 10 nM 4-IBP for 48 to 96 hours induced weak, if any, apoptosis-related PARP cleavage. Flow cytometry analyses of TUNEL staining confirmed the absence of 4-IBP–induced apoptotic features at 10 and 100 nM in U373-MG cells (data not shown). Figure 4*Eb* shows that the levels of expression of p53 protein in untreated U373-MG cells were high and that 10 nM 4-IBP did not modify this expression.

4-IBP Does Not Induce Autophagy in Human U373-MG Glioblastoma Cells

As shown by the use of acridine orange staining (Figure 5*A*), the treatment of U373-MG cells for 72 hours with increasing concentrations of 4-IBP did not induce any significant ($P > .05$) increase in the percentages of acidic compartments. Such acidic vesicular organelles may relate to autophagic vacuoles in the cells [28,42]. The data in Figure 5, *B* and *C*, confirm those illustrated in Figure 5*A*. Indeed, even at high concentrations (10 μM), 4-IBP did not increase markedly the levels of expression of LC3 and Beclin-1, two specific markers of autophagy [28,42]. Modifications to the percentage of acridine orange staining in tumor cells may also relate to lysosomal membrane permeabilization (LMP), an Hsp70-dependent process [43] that may be indicative of the leakage of acridine orange from the acidic compartment to the cytosol [43]. The data in Figure 5*D* show that 4-IBP (up to 10 μM) did not markedly modify the levels of expression of Hsp70.

4-IBP Does Not Interfere with Responses to Endoplasmic Reticulum Stress (ERS)

ERS arises from the fact that cancer cells in poorly vascularized solid tumors (including GBMs) are constantly or intermittently exposed to nutrient and glucose deprivation, hypoxia, redox and glycosylation reactions, and disturbances in calcium mobilization [44,45]. Under such conditions, eukaryotic cells normally respond through at least three different mechanisms, namely, transcriptional induction, translational attenuation, and degradation (ER-associated degradation) [44–46]. Transcriptional induction derives from the activation of an intracellular signaling pathway from the ER to the nucleus, which is known as unfolded protein response (UPR) [44,46]. Excessive or long-term stress in the ER results in apoptotic cell death involving nuclear fragmentation, chromatin condensation, and cell body shrinkage [44]. A lower level of susceptibility to cell death on the activation of the UPR may contribute to tumor progression and drug resistance of solid tumors [44]. Thus, the inhibition of the UPR might

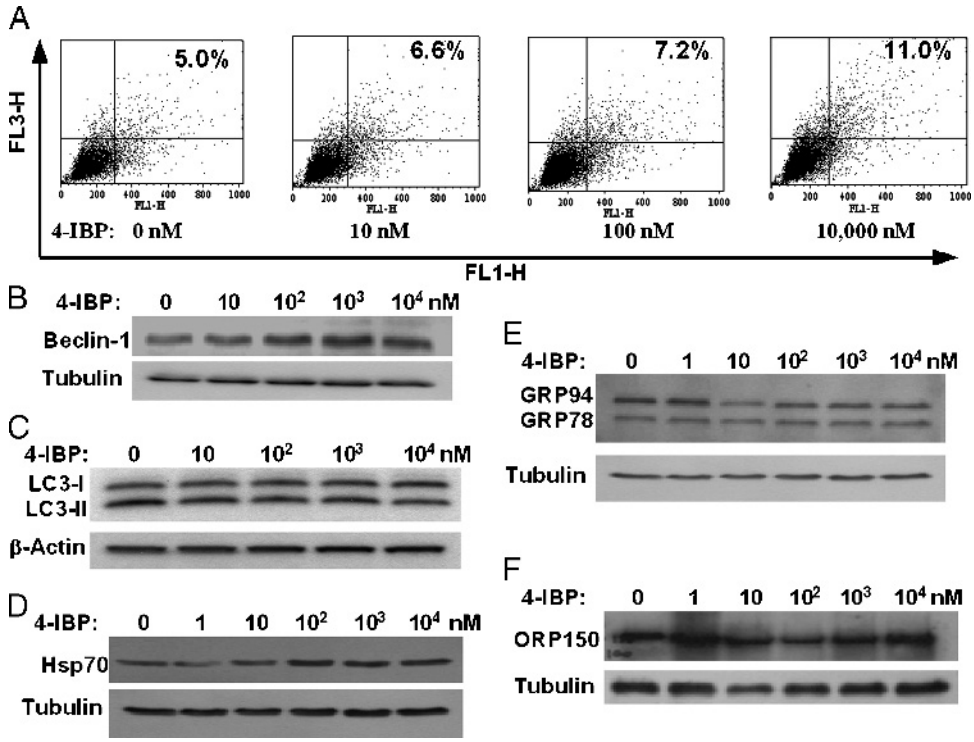

Figure 5. *(A) The detection and quantification of acidic vesicular organelles by acridine orange staining using flow cytometry in human U373-MG GBM cells treated for 72 hours with increasing concentrations of 4-IBP. In acridine orange–stained cells, the cytoplasm and nucleus fluoresce green (y-axis), whereas acidic compartments fluoresce red (x-axis). The intensity of the red fluorescence is proportional to the degree of acidity and to the volume of acidic vesicular organelles, including autophagic vacuoles. The values in (A) refer to the percentages of cells with a significant proportion of acidic vesicular organelles. (B–F) Western blot analyses of Beclin-1 (B); microtubule-associated protein 1 LC3 (an autophagosomal orthologue of yeast Atg8/Aup7) type I (LC3-I) and type II (LC3-II) (C); Hsp70 (D); GRP78 (E); and ORP150 (F) in human U373-MG glioblastoma cells treated with increasing concentrations of 4-IBP for 72 hours.*

improve the effectiveness of chemotherapy [44]. ER chaperones, such as GRP78 and Gadd153, play a number of critical roles in cell survival and cell death as part of the UPR [44]. GRP78 is also involved in cancer cell resistance to cytotoxic drugs [47]. ORP150 is also a component of the ERS response to hypoxia, potentially facilitating protein processing [46]. ORP150 was first identified and cloned from cultured astrocytes based on their ability to withstand and even produce neurotrophic factors in response to severe hypoxia [46]. The expression of ORP150 in cultured human cells is essential for their survival under prolonged hypoxia [46]. Because GRP78 and ORP150 are major players in the ERS responses of cancer cells to cytotoxic agents [44–47], an investigation was undertaken to ascertain whether 4-IBP could modify their levels of expression in human U373-MG GBM cells. The data in Figure 5*E* show that even at high concentrations (10 μM), 4-IBP did not modify the levels of expression of GRP78. The same observation was made in the case of Gadd153 (data not shown). In the same way, the data in Figure 5*F* show that 4-IBP did not modify the levels of expression of ORP150 in human GBM cells. Taken together, these data suggest that it is unlikely that the 4-IBP–mediated sensitization of U373-MG GBM cells to the proapoptotic effects of lomustin (Figure 4*A*) or proautophagic effects of temozolomide (Figure 4*B*) relates to induced modification to ERS.

4-IBP Markedly Reduces the Levels of Expression of Rho GDI and GCS in U373-MG GBM Cells

The failure to evidence any 4-IBP–mediated influence on proapoptotic (Figure 4, *C–E*), proautophagic (Figure 5, *A–C*), pro-LMP (Figure 5, *A* and *D*), or pro-ERS responses (Figure 5, *E* and *F*) prompted the treatment of U373-MG GBM cells with 10 nM 4-IBP for 12 hours, followed by a genomewide microarray analysis of treated cells, to try and elucidate how the compound sensitizes these glioblastoma cells to the cytotoxic insults of lomustin and temozolomide (Figure 4, *A* and *B*). Genomic analysis revealed that the two genes whose levels were most heavily modified in these 4-IBP–treated cells (30–50% decrease in their expression compared to controls) were *Rho GDI* and *GCS*. *Rho GDI* and *GCS* are genes known to be involved in drug resistance [48–50]. Immunofluorescence analyses confirmed these data at the proteomic level. Figure 6*A* shows a concentrated and perinuclear site for Rho GDI in U373-MG GBM untreated cells. This site became diffuse when these cells were treated for 72 hours with 1 nM 4-IBP (Figure 6*B*), and Rho GDI expression was almost completely abolished when the cells were treated for 72 hours with 10 nM 4-IBP (Figure 6*C*). The treatment of U373-MG GBM cells with 1 and 10 nM 4-IBP for 72 hours also produced similar effects in the case of GCS expression (Figure 6, *E* and *F*), which again was almost completely abolished at the higher 4-IBP concentration compared to controls (Figure 6*D*).

In Vivo *Characterization of 4-IBP–Induced Effects on the Survival of Immunodeficient Mice Bearing Orthotopic U373-MG Glioblastoma or A549 NSCLC Xenografts*

4-IBP significantly (P = .03) increased the survival of orthotopic U373-MG GBM xenograft-bearing mice and also significantly (P = .02) increased the therapeutic benefit of

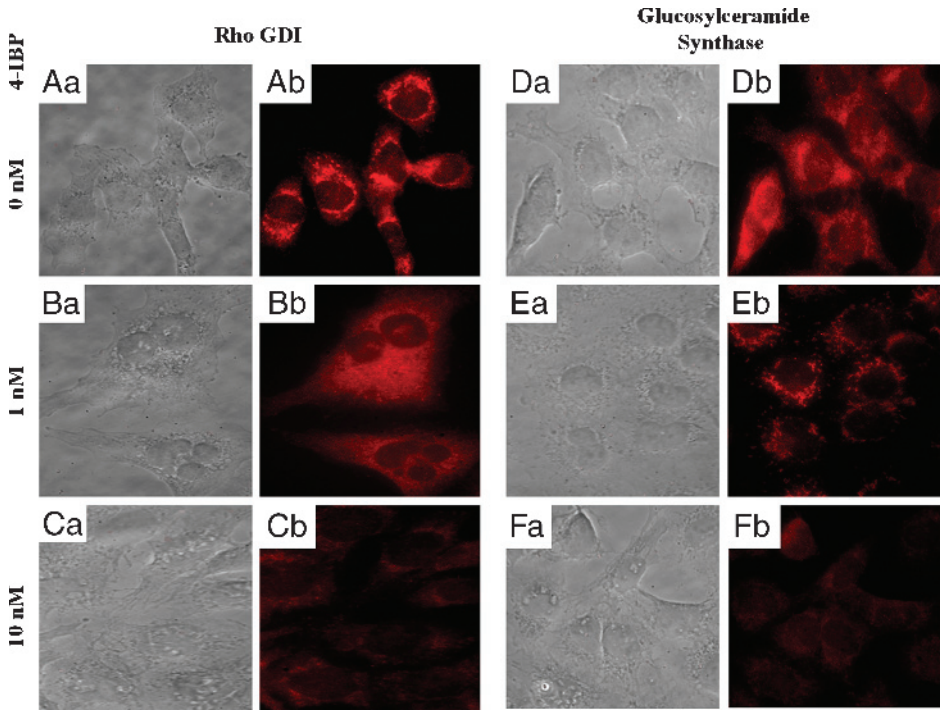

Figure 6. *Immunofluorescence analyses in the investigation of the expression of Rho GDI (A–C) and GCS (D–F) in U373-MG GBM cells left untreated (A and D) or treated for 72 hours with 1 nM 4-IBP (B and E) and 10 nM 4-IBP (C and F). The levels of expression of Rho GDI and GCS are shown as red fluorescence (right panels), with bright-field microscope analysis (left panels) as morphologic control.*

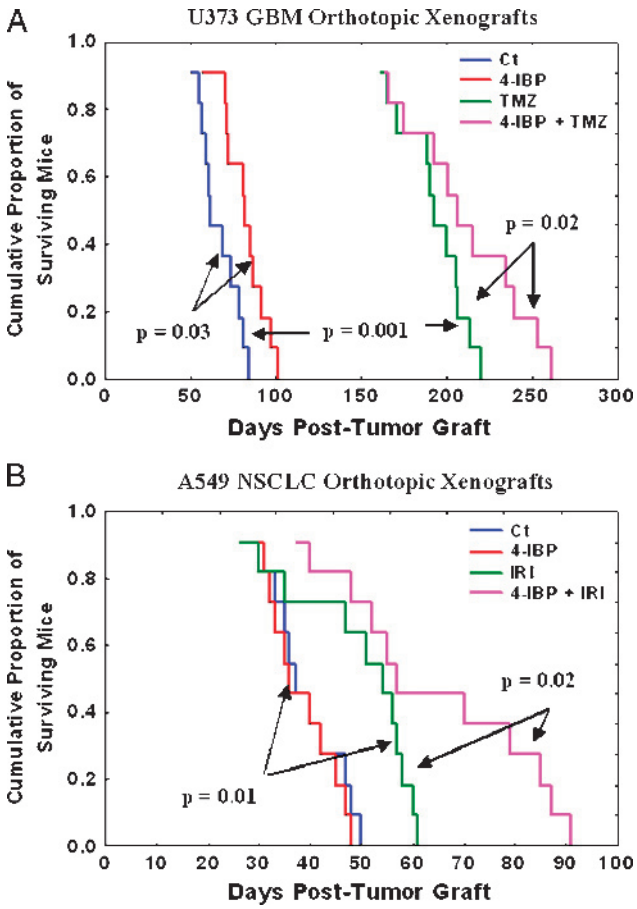

Figure 7. *(A) The survival of mice orthotopically (brain) grafted with human U373-MG GBM cells after treatment with 4-IBP alone (red line) or combined with temozolomide (purple line), compared to temozolomide alone (green line) and controls (blue line). (B) The survival of mice orthotopically (lung) grafted with human A549 NSCLC cells after treatment with 4-IBP alone (red line) or combined with IRI (purple line), compared to IRI alone (green line) and controls (blue line).*

temozolomide (Figure 7*A*). In the same manner, 4-IBP significantly (P = .02) increased the therapeutic benefits contributed by IRI in the A549 NSCLC orthotopic xenograft model, whereas it was unable *per se* to augment significantly the survival of A549 NSCLC-bearing mice (Figure 7*B*). Although IRI is not the first choice for lung cancer, we nevertheless chose it because it is the only cytotoxic drug that displayed previously therapeutic benefits in the A549 NSCLC orthotopic model [36].

Discussion

Although there is considerable evidence for the involvement of σ receptors in cancer cell biology, the mechanism(s) through which these implications occur has not fully been identified [4]. In fact, σ_1 receptors and/or σ_1 drugs could produce their anticancer effects by modulating ion channels such as high-voltage–activated Ca^{2+} channels, including N, L, P/Q, and R types, and voltage-gated K^+ channels [4]. In their recent review of the potential involvement of σ receptors in cancer biology, Aydar et al. [4] report that, to date, studies on the σ_1 receptor modulation of K^+ channels have deduced that the signal transduction mechanism of σ_1 receptors: 1) is membrane-bound; 2) is independent of G-protein coupling and protein phosphorylation; 3) can be reconstituted in a heterogenous system; and 4) does not require cytoplasmic factors but 5) does require the σ_1 receptor and the K^+ channel to be in close proximity, in all probability to form a stable macromolecular complex.

The data from the present study have demonstrated through the use of a selective σ_1 receptor agonist 4-IBP the involvement of σ_1 receptors in cancer cell migration and the sensitization of cancer cells to cytotoxic insults from proapoptotic and proautophagic drugs, at least in human U373-MG GBM cells. These two processes may well be connected, as explained below.

It has been postulated that σ_1 receptors may play a role in the organization of the actin cytoskeleton by controlling the functioning of cytoskeletal proteins such as ankyrins, which are cytoskeletal adaptor proteins that control Ca^{2+} efflux at IP3R-3 on the endoplasmic reticulum [51]. Whereas we observed that 4-IBP modifies the organization of the actin cytoskeleton in human U373-MG glioblastoma cells, no corresponding changes to $[Ca^{2+}]_i$ were observed in these cells.

Cancer cell migration, a hallmark of glioma cell biology [52,53], is the biologic process that ultimately leads to the development of metastases (excepted in gliomas), and about 90% of cancer patients die from their metastases. Migrating cancer cells are resistant to apoptosis [21,22], and a majority of anticancer drugs used to treat cancer patients are pro-apoptotic agents and thus are weakly effective against metastases [21]. The acquisition of resistance to apoptosis is essential for cancers to develop and progress, and is a major reason behind treatment failures [19]. In fact, cancer cells undergo clonal unrestrained proliferation, transgress normal tissue boundaries, and migrate to distant parts [19]. To disregard microenvironmental constraints in this way, tumor cells must acquire resistance to apoptosis [19,21,22] or they will die when deprived of the support of familiar neighbors [19,21,22]. Spruce et al. [19] have shown that small molecule antagonists of the σ_1 receptor inhibit tumor cell survival and induce caspase-dependent apoptosis. Although several normal cell types, such as fibroblasts, epithelial cells, and even σ receptor–rich neurons, are resistant to the apoptotic effects of antagonists, cells that can promote autocrine survival, such as lens epithelial and microvascular endothelial cells, are as susceptible as tumor cells [19]. Cell susceptibility appears to correlate with differences in σ_1 receptor coupling rather than with levels of expression [19]. Only in the case of susceptible cells do σ_1 antagonists evoke a rapid rise in cytosolic calcium that is inhibited by σ_1 agonists [19]. The present study has revealed that U373-MG glioblastoma cells, which contain only variant 1 of the σ_1 receptor (Figure 1), are not susceptible to 4-IBP, which is an agonist, not an antagonist, of the σ_1 receptor. In addition, it must be emphasized that all *in vitro* data reported by Spruce et al. [19] with respect to the apoptotic features induced by σ_1 receptor antagonists were observed with such antagonists

only when used in the micromolar range, whereas our data on the effects of the σ_1 receptor agonist 4-IBP on cancer cell migration are based on nanomolar concentrations.

Whereas U373-MG GBM cells are resistant to apoptosis [32] (manuscript in preparation), the fact that low concentrations of 4-IBP modulate both migration and sensitivity to proapoptotic and proautophagic cytotoxic insults in these cells could be at least partly explained by the fact that these low concentrations also markedly decrease the levels of expression of Rho GDI in U373-MG GBM cells (Figure 6). In fact, Rho GDI plays an essential role in controlling a variety of cellular functions through interactions with Rho family GTPases, including Rac1, Cdc42, and RhoA [48]. Zhang et al. [48] have shown that the Rho GDI widely expressed in hematopoietic cells (D4-GDI) is also expressed in a panel of breast cancer cell lines, but not in benign-derived mammary epithelial cells, and that the knockdown of this protein's expression blocks cell motility and invasion. Rho GDI is also frequently overexpressed in different human tumors and chemoresistant cancer cell lines, further suggesting that it might play a role in the development of drug resistance in cancer cells [48,54]. It has also been proven that Rho GDI expression is a predictive marker of paclitaxel resistance not only in paclitaxel-resistant ovarian cancer cell lines but also in clinical samples [54]. Zhang et al. [48] observed that the overexpression of Rho GDI increases the resistance of cancer cells to the induction of apoptosis by etoposide and doxorubicin. Conversely, the silencing of Rho GDI expression by DNA vector–mediated RNA interference (small interfering RNA) sensitizes tumor cells to drug-induced apoptosis [48].

The overexpression of GCS, a pivotal enzyme in glycolipid biosynthesis, also contributes to cancer cell resistance to chemotherapy [49,50]. The present study revealed that 10 nM 4-IBP noticeably reduced the levels of expression of GCS in human U373-MG GBM cells (Figure 6). Using a series of drug-resistant human epidermoid carcinoma, breast, leukemia, melanoma, and colon cancer cell lines developed through selection pressure cloning with various anticancer drugs (adriamycin, vincristine, etoposide, and doxorubicin), Gouazé et al. [49,50] observed that increases in drug resistance are accompanied by increases in the expression and activity of GCS. These authors show that limiting GCS activity by antisense transfection or chemical inhibition restores cell chemosensitivity and downregulates the expression of MDR1, a phenomenon that may drive chemosensitization associated with blocking ceramide metabolism [49].

Given its ability to sensitize cancer cells to cytotoxic agents *in vitro*, 4-IBP was found to significantly increase the survival of orthotopic U373-MG GBM xenograft-bearing mice and the therapeutic benefit of proautophagic temozolomide. 4-IBP also significantly increased the therapeutic benefits contributed by proapoptotic IRI in the A549 NSCLC orthotopic xenograft model, whereas it was unable *per se* to augment significantly the survival of A549 NSCLC-bearing mice.

In conclusion, activating the σ_1 receptor with noncytotoxic doses of the σ_1 receptor agonist 4-IBP decreases the migration levels of various types of cancer cells, including C32 melanoma, U373-MG glioblastoma, A549 NSCLC, and PC3 prostate cancer cells. This activation in U373-MG glioblastoma cells displaying the σ_1 receptor V1 transcript variant only leads to their sensitization to proapoptotic or proautophagic cytotoxic insults, a process in which Rho GDI and GCS seem to be involved.

Acknowledgement

We thank Vincenzo Facchini for his support during the review of this manuscript.

References

[1] Su TP (1993). Delineating biochemical and functional properties of sigma receptors: emerging concepts. *Crit Rev Neurobiol* **7**, 187–203.

[2] Walker JM, Hohmann AG, and Hemstreet MK (1993). Functional role of sigma receptors in the nervous system. In TW Stone (Ed.). Aspects of Synaptic Transmission. Taylor and Francis, Washington, DC, pp. 91–112.

[3] Whittemore ER, Ilyin VI, and Woodward RM (1997). Antagonism of *N*-methyl-D-aspartate receptors by σ site ligands: potency, subtype-selectivity and mechanisms of inhibition. *J Pharmacol Exp Ther* **282**, 326–338.

[4] Aydar E, Palmer CP, and Djamgoz BA (2004). Sigma receptors and cancer: possible involvements of ion channels. *Cancer Res* **64**, 5029–5035.

[5] Bowen WD (2000). Sigma receptors: recent advances and new clinical potentials. *Pharm Acta Helv* **74**, 211–218.

[6] Bourrie B, Bribes E, Derocq JM, Vidal H, and Casellas P (2004). Sigma receptor ligands: applications in inflammation and oncology. *Curr Opin Invest Drugs* **5**, 1158–1163.

[7] Vilner BJ, John CS, and Bowen WD (1995). Sigma-1 and sigma-2 receptors are expressed in a wide variety of human and rodent tumor cell lines. *Cancer Res* **55**, 408–413.

[8] Martin W, Eades C, Thompson J, Huppler R, and Gilbert P (1976). The effects of morphine- and nalorphine-like drugs in the non-dependent and morphine-dependent chronic spinal dog. *J Pharmacol Exp Ther* **197**, 517–532.

[9] Quirion R, Bowen W, Itzhak Y, Junien JL, Musacchio JM, Rothman RB, Su TP, Tam SW, and Taylor DP (1992). A proposal for the classification of sigma binding sites. *Trends Pharmacol Sci* **13**, 85–86.

[10] Bermack JE and Debonnel G (2001). Modulation of serotonergic neurotransmission by short- and long-term treatments with sigma ligands. *Br J Pharmacol* **134**, 691–699.

[11] Vidal H, Mondesert G, Galiègue S, Carriere D, Dupuy PH, Carayon P, Combes T, Bribes E, Simony-Lafontaine J, Kramar A, et al. (2003). Identification and pharmacological characterization of SRBP-2: a novel SR31747A-binding protein. *Cancer Res* **63**, 4809–4818.

[12] Hanner M, Moebius FF, Flandorfer A, Knaus HG, Striessnig J, Kempner E, and Glossmann H (1996). Purification, molecular cloning and expression of the mammalian sigma$_1$-binding site. *Proc Natl Acad Sci USA* **93**, 8072–8077.

[13] Kekuda R, Prasad PD, Fei YJ, Leibach FH, and Ganapathy V (1996). Cloning and functional expression of the human type 1 sigma receptor (hSigmaR1). *Biochem Biophys Res Commun* **229**, 553–558.

[14] John CS, Bowen WD, Fisher SJ, Lim BB, Geyer BC, Vilner BJ, and Wahl RL (1999). Synthesis, *in vitro* pharmacological characterization and preclinical evaluation of *N*-(2-(1′piperidinyl)ethyl)-3-(^{125}I)iodo-4-methoxybenzamide (P(^{125}I)MBA) for imaging breast cancer. *Nucl Med Biol* **26**, 377–382.

[15] Brent PJ and Pang GT (1995). Sigma binding site ligands inhibit cell proliferation in mammary and colon carcinoma cell lines and melanoma cells in culture. *Eur J Pharmacol* **278**, 151–160.

[16] Vilner BJ, de Costa BR, and Bowen WD (1995). Cytotoxic effects of sigma ligands: sigma receptor–mediated alterations in cellular morphology and viability. *J Neurosci* **15**, 117–134.

[17] Brent PJ, Pang G, Little G, Dosen PJ, and Van Helden DF (1996). The sigma receptor ligand, reduced haloperidol, induces apoptosis and increases intracellular-free calcium levels [Ca^{2+}]$_i$ in colon and mammary adenocarcinoma cells. *Biochem Biophys Res Commun* **219**, 219–226.

[18] Moody TW, Leyton J, and John C (2000). Sigma ligands inhibit the growth of small cell lung cancer cells. *Life Sci* **66**, 1979–1986.

[19] Spruce BA, Campbell LA, McTavish N, Cooper MA, Appleyard MV, O'Neill M, Howie J, Samson J, Watt S, Murray K, et al. (2004). Small molecule antagonists of the σ-1 receptor cause selective release of the death program in tumor and self-reliant cells and inhibit tumor growth *in vitro* and *in vivo*. *Cancer Res* **64**, 4875–4886.

[20] Crawford KW, Coop A, and Bowen WD (2002). Sigma (2) receptors regulate changes in sphingolipid levels in breast tumor cells. *Eur J Pharmacol* **443**, 207–209.

[21] Decaestecker C, Debeir O, Van Ham P, and Kiss R (2007). Can anti-migratory drugs be screened *in vitro*? A review of 2D and 3D assays for the quantitative analysis of cell migration. *Med Res Rev* **27**, 149–176.

[22] Lefranc F, Brotchi J, and Kiss R (2005). Possible future issues in the treatment of glioblastomas: special emphasis on cell migration and the resistance of migrating glioblastoma cells to apoptosis. *J Clin Oncol* **23**, 2411–2422.

[23] Bermack JE and Debonnel G (2005). Distinct modulatory roles of sigma receptor subtypes on glutamatergic responses in the dorsal hippocampus. *Synapse* **55**, 37–44.

[24] Anderson TR and Andrew RD (2002). Spreading depression: imaging and blockade in the rat neocortical brain slice. *J Neurophysiol* **88**, 2713–2725.

[25] John CS, Vilner BJ, and Bowen WD (1994). Synthesis and characterization of [^{125}I]-*N*-(*N*-benzylpiperidin-4-yl)-4-iodobenzamide, a new sigma receptor radiopharmaceutical: high-affinity binding to MCF7 breast tumor cells. *J Med Chem* **37**, 1737–1739.

[26] Mathieu V, Mijatovic T, Van Damme M, and Kiss R (2005). Gastrin exerts pleiotropic effects on human melanoma cell biology. *Neoplasia* **7**, 930–943.

[27] Prasad PD, Li HW, Fei YJ, Ganapathy ME, Fujita T, Plumley LH, Yang-Feng TL, Leibach FH, and Ganapathy V (1998). Exon–intron structure, analysis of promoter region, and chromosomal localization of the human type 1 sigma receptor gene. *J Neurochem* **70**, 443–451.

[28] Mijatovic T, Mathieu V, Gaussin JF, De Neve N, Ribaucour F, Van Quaquebeke E, Dumont P, Darro F, and Kiss R (2006). Cardenolide-induced lysosomal membrane permeabilization demonstrates therapeutic benefits in experimental human non–small cell lung cancers. *Neoplasia* **8**, 402–412.

[29] Kanzawa T, Germano IM, Komata T, Ito H, Kondo Y, and Kondo S (2004). Role of autophagy in temozolomide-induced cytotoxicity for malignant glioma cells. *Cell Death Differ* **11**, 448–457.

[30] Debeir O, Van Ham P, Kiss R, and Decaestecker C (2005). Tracking of migrating cells under phase-contrast video microscopy with combined mean-shift processes. *IEEE Trans Med Imaging* **24**, 697–711.

[31] Lefranc F, Mijatovic T, Mathieu V, Rorive S, Decaestecker C, Debeir O, Brotchi J, Van Ham P, Salmon I, and Kiss R (2004). Characterization of gastrin-induced pro-angiogenic effects *in vivo* in orthotopic U373 experimental human glioblastomas and *in vitro* in human umbilical vein endothelial cells. *Clin Cancer Res* **10**, 8250–8265.

[32] Vandenbrouck C, Martin D, Colson-Van Schoor M, Debaix H, and Gailly P (2002). Involvement of TRPC in the abnormal calcium influx observed in dystrophic (mdx) mouse skeletal muscle fibers. *J Cell Biol* **158**, 1089–1096.

[33] Branle F, Lefranc F, Camby I, Jeuken J, Geurts-Moespot A, Sprenger S, Sweep F, Kiss R, and Salmon I (2002). Evaluation of the efficiency of chemotherapy in *in vivo* orthotopic models of human glioma cells with and without 1p19q deletions and in C6 rat orthotopic allografts serving for the evaluation of surgery combined with chemotherapy. *Cancer* **95**, 641–655.

[34] Stupp R, Mason WP, van den Bent MJ, Weller M, Fisher B, Taphoorn MJ, Belanger K, Brandes AA, Marosi C, Bogdahn U, et al. (2005). Radiotherapy plus concomitant and adjuvant temozolomide for glioblastoma. *N Engl J Med* **4** (352), 987–996.

[35] Lefranc F, Sadeghi N, Metens T, Brotchi J, Salmon I, and Kiss R (2003). Characterization of gastrin-induced cytostatic effect on cell proliferation in experimental malignant gliomas. *Neurosurgery* **52**, 881–890.

[36] Mathieu A, Remmelink M, D'Haene N, Penant S, Gaussin JF, Van Ginckel R, Darro F, Kiss R, and Salmon I (2004). Development of a chemoresistant orthotopic human non small cell lung carcinoma model in nude mice. *Cancer* **101**, 1908–1918.

[37] Friedl P and Wolf K (2003). Cell–cell invasion and migration: diversity and escape mechanisms. *Nat Rev Cancer* **3**, 362–374.

[38] Furuyashiki T, Arakawa Y, Takemoto-Kimura S, Bito H, and Narumiya S (2002). Multiple spatiotemporal modes of actin reorganization by NMDA receptors and voltage-gated Ca^{2+} channels. *Proc Natl Acad Sci USA* **99**, 14458–14463.

[39] Feldner JC and Brandt BH (2002). Cancer cell motility—on the road from c-erb-2 receptor steered signaling to actin reorganization. *Exp Cell Res* **272**, 93–108.

[40] Lefranc F, James S, Camby I, Gaussin JF, Darro F, Brotchi J, Gabius HJ, and Kiss R (2005). Combined cimetidine and temozolomide, compared with temozolomide alone: significant increases in survival in nude mice bearing U373 human glioblastoma multiforme orthotopic xenografts. *J Neurosurg* **102**, 706–714.

[41] Maleniak TC, Darling JL, Lowenstein PR, and Castro MG (2001). Adenovirus-mediated expression of HSV1-TK or Fas ligand induces cell death in primary human glioma–derived cell cultures that are resistant to the chemotherapeutic agent CCNU. *Cancer Gene Ther* **8**, 589–598.

[42] Kondo Y, Kanzawa T, Sawaya R, and Kondo S (2005). The role of autophagy in cancer development and response to therapy. *Nat Rev Cancer* **5**, 726–734.

[43] Kroemer G and Jäättelä M (2005). Lysosomes and autophagy in cell death control. *Nat Rev Cancer* **5**, 886–897.

[44] Kim R, Emi M, Tanabe K, and Murakami S (2006). Role of the unfolded protein response in cell death. *Apoptosis* **11**, 5–13.

[45] Shannon AM, Bouchier-Hayes DJ, Condron CM, and Toomey D (2003). Tumour hypoxia, chemotherapeutic resistance and hypoxia-related therapies. *Cancer Treat Rev* **29**, 297–307.

[46] Ozawa K, Tsukamoto Y, Hori O, Kitao Y, Yanagi H, Stern DM, and Ogawa S (2001). Regulation of tumor angiogenesis by oxygen-regulated protein 150, an inducible endoplasmic reticulum chaperone. *Cancer Res* **61**, 4206–4213.

[47] Li J and Lee AS (2006). Stress induction of GRP78/BiP and its role in cancer. *Curr Mol Med* **6**, 45–54.

[48] Zhang B, Zhang Y, Dagher MC, and Shacter E (2005). Rho GDP dissociation inhibitor protects cancer cells against drug-induced apoptosis. *Cancer Res* **65**, 6054–6062.

[49] Gouazé V, Liu YY, Prickett CS, Yu JY, Giuliano AE, and Cabot MC (2005). Glucosylceramide synthase blockade down-regulates P-glycoprotein and resensitizes multidrug-resistant breast cancer cells to anticancer drugs. *Cancer Res* **65**, 3861–3867.

[50] Gouazé V, Yu JY, Bleicher RJ, Han TY, Liu YY, Wang H, Gottesman MM, Bitterman A, Giuliano AE, and Cabot MC (2004). Over-expression of glucosylceramide synthase and P-glycoprotein in cancer cells selected for resistance to natural product chemotherapy. *Mol Cancer Ther* **3**, 633–639.

[51] Hayashi T and Su TP (2001). Regulating ankyrin dynamics roles of sigma-1 receptors. *Proc Natl Acad Sci USA* **98**, 491–496.

[52] McDonough WS, Tran NL, and Berens ME (2005). Regulation of glioma cell migration by serine-phosphorylated P311. *Neoplasia* **7**, 862–872.

[53] Lipinski CA, Tran NL, Menashi E, Rohl C, Kloss J, Bay RC, Berens ME, and Loftus JC (2005). The tyrosine kinase Pyk2 promotes migration and invasion of glioma cells. *Neoplasia* **7**, 435–445.

[54] Goto T, Takano M, Sakamoto M, Kondo A, Hirata J, Kita T, Tsuda H, Tenjin Y, and Kikuchi Y (2006). Gene expression profiles with cDNA microarray reveal Rho GDI as a predictive marker for paclitaxel resistance in ovarian cancers. *Oncol Rep* **15**, 1265–1271.